

The Weakest Link

Degradation of a weld through interaction with hydrogen

Jonas Cop
Charlot Depestel
Nathalie Saikali
Sharon Temmerman
Dorien Zeebroek

Department of Materials, Textiles and
Chemical Engineering (MaTCh)
Faculty of Engineering and Architecture
Ghent University, BELGIUM
Kim.Verbeke@UGent.be

ABSTRACT

This work evaluates the effect of hydrogen on welds in martensitic steels. In-situ constant-load tensile testing of a weld of HB450 steel shows that hydrogen-induced cracks appear in the filler material, which is capable of trapping the highest amount of hydrogen, as indicated by thermal desorption spectroscopy (TDS). Further crack propagation takes place in the part of the heat affected zone (HAZ) with the highest hardness.

Keywords

Welding; hydrogen-induced cracking

INTRODUCTION

Hydrogen is inescapable in our daily environment due to its presence in hydrocarbons, among others present in coatings and lubricants, or simply due to its presence in the moisture of the air. Additionally, cathodic corrosion protection relies on electrochemical reactions which can cause the production of hydrogen at the material's surface. Hydrogen can have a detrimental impact on the mechanical integrity of materials, such as by hydrogen-induced cracking (HIC) [1, 2].

Hydrogen-induced cracking is caused by the sequence of several processes. First, hydrogen adsorbs on the surface, after which it absorbs in the material and diffuses through the material towards stress concentrations. There, hydrogen atoms recombine to hydrogen gas molecules, causing internal pressure and thus internal stresses. When this pressure trespasses a critical value, cracks can initiate and propagate throughout the material. In order to take place, certain requirements must be fulfilled:

- Sufficient amount of hydrogen
- Sufficient stress
- Susceptible microstructure

Today, welding (and other joining technologies) is a matter of the uttermost importance. It is essential in plenty of disciplines, such as in construction or in the automotive industry. About 70% of all manufactured products have undergone some form of welding [3]. The welding process is very sensitive to hydrogen introduction due to the high temperatures involved. Since welded structures often are key pieces in a construction, the need of strong and trustworthy welds and general knowledge is crucial. The purpose of this paper is to find the weakest link, i.e. the location of the first cracks due to hydrogen interaction, in a weld and its heat affected zone (HAZ).

EXPERIMENTAL PROCEDURE

Material characterization

For this study, HARDOX HB450 was used, a commercially available martensitic steel. Its composition is given in Table 1. A weld of this material was obtained by a Metal Active Gas (MAG) welding process, using a mixture of Ar and CO₂ gas and LNM MoNiCr as filler material.

Table 1: Chemical composition of HARDOX 450 HB in wt%.

Element	C	Mn	Si	P
Wt%	0.188	1.463	0.488	0.013
Element	S	Ni	Cr	Cu
Wt%	0.001	0.034	0.327	0.023

In order to analyze each zone of the weld separately, welding simulations were made based on the welding parameters [4]. For this, thermocouples were placed in the material during welding and for each zone, the corresponding T_{8/5} was determined. This is the time it takes for the metal to cool down from 800 °C to 500 °C. In this temperature range, the austenitic phase, which was formed during the heating of the material, undergoes a phase transformation.

Microstructural characterization was first performed using light optical microscopy (LOM) on a Keyence VHX-S90BE microscope. The samples for LOM were prepared by conventional grinding and polishing, followed by etching with Nital 2% for 20 seconds. Further characterization was performed with scanning electron microscopy (SEM), for which a FEI Quanta 450 SEM with field emission gun was used. The SEM was operated at an acceleration voltage of 20 kV and a spot size of 5 nm.

Vickers hardness (HV) measurements were performed in order to establish a hardness profile through the weld. These tests were done using a Zwick hardness tester with pyramidic diamond cone with a weight of 3 kg and a loading time of 10 s.

Hydrogen/material interaction

In order to evaluate the amount of hydrogen present in each part of the weld, thermal desorption spectroscopy (TDS) was used on a Bruker Galileo G8 ON/H. Samples for TDS were first electrochemically charged for 2 h in a 0.5M H₂SO₄ solution with 1 g/l thiourea at a current density of 0.8 mA/cm². The samples were then heated to 900 °C at a heating rate of 1200 °C/h. Upon heating, the hydrogen is released from the sample and sent to a quadrupole mass spectrometer. After calibration, it is possible to correlate the measured amount of hydrogen to the concentration of hydrogen in the metallic sample.

Hydrogen-induced damage

The hydrogen-induced damage was determined by performing in-situ constant-load tensile tests under the same hydrogen charging conditions as described in the previous section. Before the in-situ constant-load test, the sample was electrochemically charged for 2 h. In-situ constant-load tensile tests were then performed on a 5800R electro-mechanical Instron at a strain rate of 10^{-4} s^{-1} until 80% of the yield stress of the weld was reached. The sample was held at this stress for 15 minutes and was subsequently polished and examined using SEM.

RESULTS AND DISCUSSION

Microstructural characterization

Figure 1 shows an optical micrograph of the weld and its heat affected zone (HAZ). Apart from the base material and the filler, two parts of heat affected zone were identified, i.e. HAZ 1 and HAZ 2.

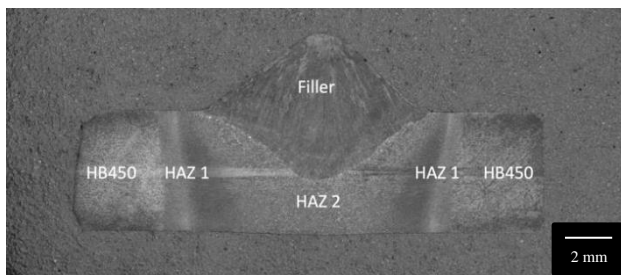


Figure 1: LOM image of the weld of base material HB450 with filler and heat affected zones HAZ 1 and HAZ 2.

Base material (HB450)

The microstructure of the base material HB450 can be seen in Figure 2. A fully martensitic material, indicated by a fine needle-like structure, was observed.

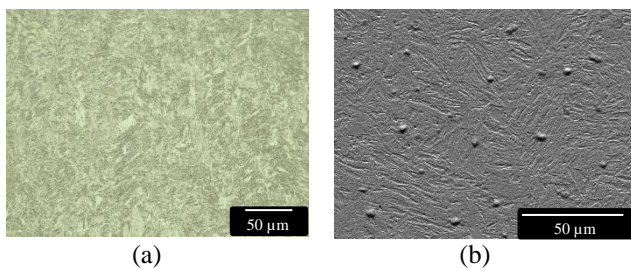


Figure 2: Representative images of HB450: (a) LOM, (b) SEM. Fully martensitic material with fine needle-like structure.

Filler

Representative images of the filler material are given in Figure 3. The chaotic structure and lenticular grains indicate the presence of acicular ferrite. During cooling down from the austenitic phase, these grains nucleated in different directions on inclusions present in the material. Due to its chaotic structure, there is a high amount of misorientation between the grains. This results in superior toughness, because of the decreased mobility of propagating cracks.

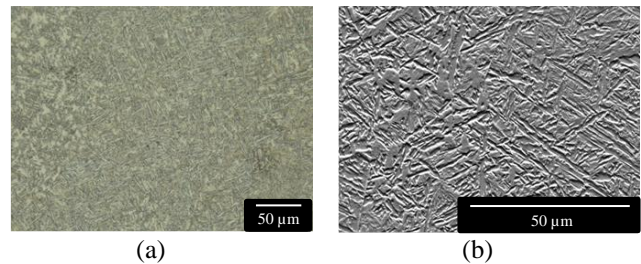


Figure 3: Representative images of the filler: (a) LOM, (b) SEM. Acicular ferritic microstructure.

Heat affected zone

The heat affected zone consisted of two parts: HAZ 1 close to the base material HB450 and HAZ 2 close to the filler. The microstructure of HAZ 1, as shown in Figure 4, is most likely tempered martensite. The temperature was not sufficiently high to transform back to austenite, since HAZ 1 was relatively far from the filler material. This will be confirmed with hardness measurements in the next section. By contrast, HAZ 2 was heated into the austenitic range and transformed into martensite upon cooling down, as indicated by the coarse needle-like structure in Figure 5.

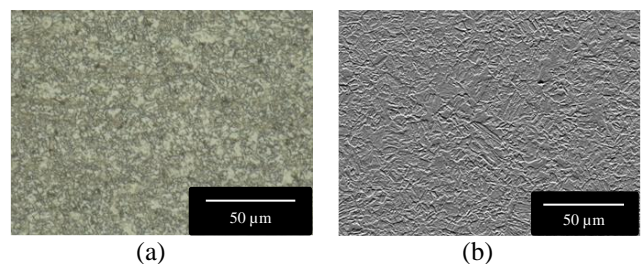


Figure 4: Representative images of HAZ 1: (a) LOM, (b) SEM. Tempered martensitic microstructure.

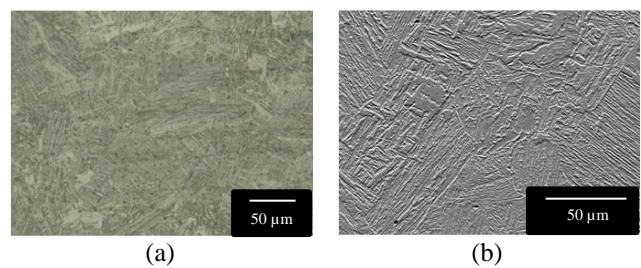


Figure 5: Representative images of HAZ 2: (a) LOM, (b) SEM. Coarse needle-like martensitic microstructure.

Hydrogen-induced damage

During the in-situ constant-load tensile test of the weld, hydrogen is allowed to diffuse to sensitive regions in the material. Due to the intensity of the load, cracks may start to form at these sensitive regions. This allows to determine where cracks can initiate and eventually propagate, leading to failure.

SEM images of the weld after the in-situ constant-load tensile test are shown in Figures 6 and 7. Small cracks were found inside the filler material, as presented in Figure 6. An overview SEM image of the weld after the in-situ constant-load tensile test is shown in Figure 7. The different sections of the heat affected zone and the direction of the tensile force are indicated on the figure as well.

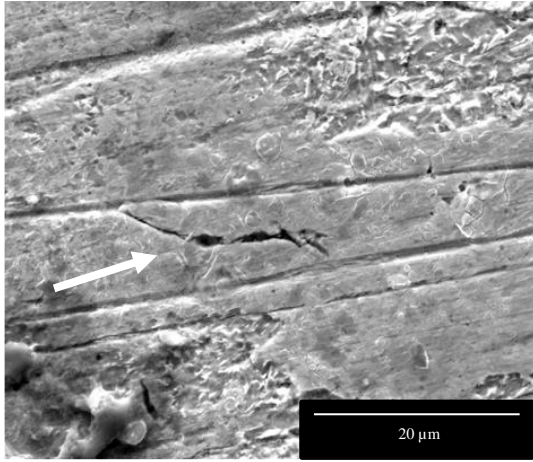


Figure 6: Hydrogen induced crack in filler material during in-situ constant-load tensile test under hydrogen charging.

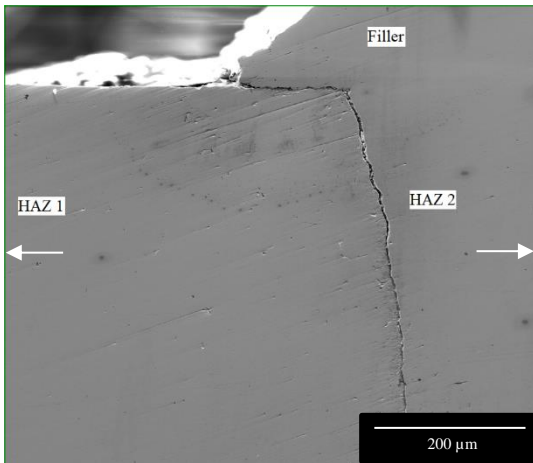


Figure 7: SEM image of the weld after in-situ constant-load tensile testing: crack initiating at the base of the filler and propagating into HAZ 2.

Evaluation on the active mechanism of H-damage

In order to determine the susceptibility of each zone to hydrogen-induced cracking, the hydrogen uptake and trapping capacity of each zone of the weld and the hardness profile along the weld were determined.

Thermal desorption spectroscopy was used to measure the hydrogen uptake and trapping capacity in the different zones. A higher hydrogen concentration implies increased solubility of hydrogen in the microstructure. The resulting TDS spectra can be found in Figure 8, with the concentration of hydrogen in the different zones given in Table 2. For all different zones of the weld, the TDS spectra show only one peak at a relatively low temperature, indicating that hydrogen was trapped at weak trapping sites, e.g. dislocations and grain boundaries, in all zones [5].

The heat affected zones contained the least amount of hydrogen, whereas the hydrogen concentration of the filler was the highest compared to the other zones. Therefore, the heat affected zones would be the most resistant to hydrogen-induced damage based on this criterion only. In contrast, the filler was most susceptible to hydrogen uptake, which explains the hydrogen induced cracks formed in the filler during the in-situ constant-load tensile test, as represented in Figure 6.

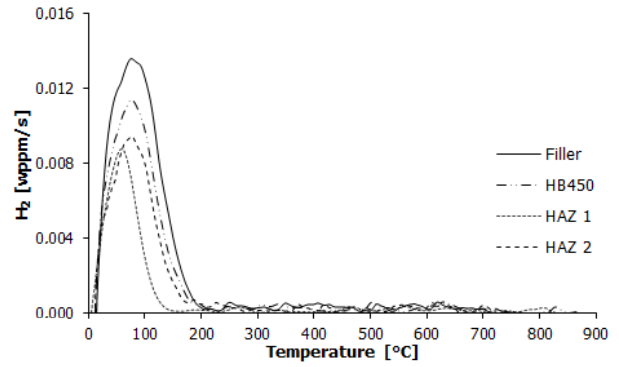


Figure 8: TDS spectra of the different zones of the weld.

Table 2: Hydrogen concentration in the different zones of the weld in wppm.

Zone	H concentration
Filler	5.40 ± 0.23
HB 450	4.30 ± 0.16
HAZ 1	2.58 ± 0.40
HAZ 2	3.39 ± 0.23

However, besides the hydrogen uptake and trapping capacity of a zone, also the hardness influences the material's behaviour towards hydrogen-induced damage. Therefore, a horizontal hardness profile was obtained, as can be seen in Figure 9. Starting from the base material, the hardness initially decreased when approaching the zone corresponding to HAZ 1. This is in accordance with the observation of a martensitic microstructure for HB450, as shown in Figure 2, and a tempered (and therefore less strong) martensitic microstructure of HAZ 1, visualized in Figure 4.

Closer to the weld, however, the hardness increased again in HAZ 2. In this zone, austenite (formed during welding) was transformed back into martensite upon cooling, as such resulting in a martensitic microstructure, as given in Figure 5. The hardness in the heat affected zone was still remarkably lower than in the base material since the cooling rate after welding was not controlled, as opposed to the cooling rate during initial production of the base material. During industrial production, the steel can be cooled significantly faster, resulting in a higher hardness of the martensite in the base material compared to HAZ 2. The higher hardness of HB450 with respect to HAZ 2 is in accordance with the observation of a fine needle-like martensitic microstructure for the base material compared to a coarse needle-like martensitic microstructure of HAZ 2, since in general a finer martensite lath thickness increases the material's hardness.

The filler material was identified to be the softest phase of all different zones of the weld. This is in accordance with the observation of an acicular ferritic microstructure, as shown in Figure 3, compared to the (tempered) martensitic microstructures of the base material and heat affected zones.

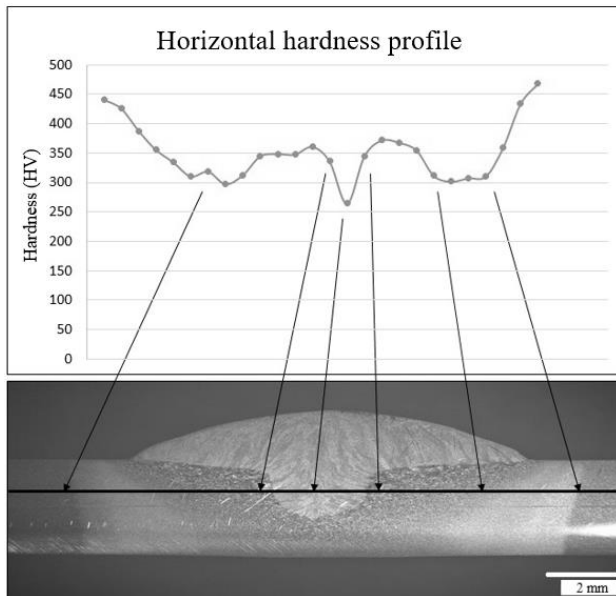


Figure 9: Horizontal hardness profile along the weld.

As can be seen in Figure 7, cracking of the weld started at the filler, despite this zone being the least brittle part of the HAZ. This can be explained by the higher amount of hydrogen in this zone, as indicated by the TDS results in Figure 8 and Table 2. This, combined with the stress concentration existing at the base of the filler, resulted in crack initiation parallel to the tensile direction along the boundary between the filler and the HAZ, as observed in Figure 7.

Further crack propagation, however, occurred perpendicular to the tensile direction as the crack deflected into the heat affected zone. More particularly, crack propagation occurred in HAZ 2, which was found to have the highest hardness of the heat affected zone, cf. Figure 9. Therefore HAZ 2 provided one of the conditions for hydrogen-induced cracking, i.e. a susceptible microstructure. Consequently, once a crack is formed, the heat affected zone acts susceptible to crack propagation.

CONCLUSION

Four different zones were identified in the weld: the base material HB450, HAZ 1, HAZ 2 and the filler. The base material had a fine martensitic structure, whereas HAZ 1 consisted of tempered martensite. The microstructure of HAZ 2 was coarse martensite, formed during welding, which had a higher hardness than HAZ 1, but lower than the base material. The filler material consisted of acicular ferrite.

The filler was capable of taking up the highest amount of hydrogen, as indicated by TDS measurements, resulting in hydrogen-induced cracks appearing in the microstructure during in-situ constant-load tensile testing.

Furthermore, when in-situ constant-load tensile testing of the weld, cracks initiated at the base of the filler. Crack propagation occurred into HAZ 2, which was the most brittle zone of the weld, based on hardness measurements.

Therefore, the filler material was the most susceptible to hydrogen-induced crack initiation, whereas HAZ 2 acted the most susceptible to crack propagation.

ROLE OF THE STUDENT

All students were specialized in a certain domain. Roughly said, Dorien, Charlot, Jonas, Nathalie and Sharon were mainly specialized in optical microscopy, SEM, TDS, in-situ constant-load tensile testing and hardness measurements, respectively. Evidently, the students helped each other whenever complications occurred. In order to come to conclusions, all knowledge was shared and discussed.

ACKNOWLEDGMENTS

We would like to thank our promotor, prof. dr. ir. Kim Verbeken, and assistants, dr. ir. Tom Depover, ir. Simon Vander Vennet and ir. Tim De Seranno, for introducing us to the subject, helping us with the practical work and advising us when encountering difficult issues.

Furthermore, we would like to thank ir. Lisa Claeys for her professional help with TDS and, last but not least, BIL (Belgian Institute for Welding) for manufacturing the initial weld and simulations.

REFERENCES

- [1] T. J. Carter and L. A. Cornish, "Hydrogen in metals," *Engineering Failure Analysis*, vol. 8, no. 2, pp. 113–121, Apr. 2001.
- [2] W. H. Johnson, "II. On some remarkable changes produced in iron and steel by the action of hydrogen and acids," *Proceedings of the Royal Society of London*, vol. 23, no. 156–163, pp. 168–179, Jan. 1875.
- [3] All State Career, "Why Welding is an Important Industry," 2019. [Online]. Available: <https://www.allstatecareer.edu/blog/skilled-trades/why-welding-is-an-important-industry.html>
- [4] WW. Pors IWE, "Warmtebehandelingen van staal vm 128," *FME-CWM, Tech. Rep.*, 2009. [Online]. Available: <https://www.induteq.nl/metaal-werktuigbouw/bestanden/VM128Wartebehandelingenvanstaal.pdf>
- [5] G. M. Pressouyre, "A classification of hydrogen traps in steel," *Metallurgical Transactions A*, vol. 10, no. 10, pp. 1571–1573, Oct. 1979.

'Permission to make digital or hard copies of all or part of this work for personal or classroom use is granted under the conditions of the Creative Commons Attribution-Share Alike (CC BY-SA) license and that copies bear this notice and the full citation on the first page''